# Synthesis and Characterization of Cu-Doped Zirconium Titanate as A Potential Visible-Light Responsive Photocatalyst

**Katarina Rachma Andita, Rian Kurniawan, and Akhmad Syoufian***

*Department of Chemistry, Faculty of Mathematics and Natural Sciences, Universitas Gadjah Mada,*
*Sekip Utara, Yogyakarta 55281, Indonesia*

* **Corresponding author:**

*email: akhmadsyoufian@ugm.ac.id*

*Received: October 18, 2018*
*Accepted: December 22, 2018*

**DOI:** 10.22146/ijc.39778

**Abstract:** *Synthesis and characterization of Cu-doped zirconium titanate as a potential visible-light responsive photocatalyst had been conducted. Titanium tetraisopropoxide (TTIP) was used as a precursor of Ti source, reacted to $ZrO_2$ powder and $CuSO_4{\cdot}5H_2O$ with various Cu concentrations of 0, 1, 3, 5, 7 and 9% (w/w) by sol-gel method. Zirconium titanate with Cu concentration of 5% was calcined at various temperatures of 500, 700 and 900 °C. All materials were characterized by using XRD, FTIR, SRUV, and SEM-EDX. The characterization proved that the materials were potential as a model of visible-light responsive photocatalyst. Composite with optimum bandgap energy ($E_g$) was obtained at 5% Cu content after 500 °C with an absorption edge wavelength of 431.93 nm and the bandgap of 2.87 eV.*

**Keywords:** *copper; dopant; Cu-doped $ZrTiO_4$; photocatalyst; sol-gel*

## ■ INTRODUCTION

Lately, there has been an increasing number of developments in photocatalyst technology. One example of photocatalyst technology usage is to decompose such as textile industrial waste. That waste contains methylene blue that is difficult to decompose naturally [1]. Titania ($TiO_2$) is a metal oxide semiconductor that has been widely studied as a photocatalyst. $TiO_2$ has relatively high redox potential, relatively high chemical stability, photo-corrosion resistance, strong oxidizing agent, economical price, and non-toxic properties. The bandgap energy of $TiO_2$ (anatase) is 3.2 eV with a UV light wavelength that is approximately $\lambda < 385$ nm [2-4]. This is the major problem of $TiO_2$ based photocatalyst under sunlight application. Only 4–5% of sunlight is in the ultraviolet region while 45% is in the visible-light region [5]. Efforts to optimize the use of sunlight are carried out by shifting $TiO_2$ uptake to the visible-light region, minimizing the $E_g$ value so that it has higher photocatalytic activity with better performance. The modification process to shift the absorption of $TiO_2$ to longer wavelength can be carried out through doping method. Doping metal ion can be transition metal cations such as $Cu^{2+}$. High recombination rate of electrons and holes in $TiO_2$ can be inhibited by the dopants as electron-trapper [6]. The reduction potential of transition metal $Cu^{2+}$ is as high as 0.34 V and Cu electronegativity being higher than Ti makes it easier to attract electrons [7].

Low $E_g$ of $TiO_2$ makes itself responsive towards the visible-light. In addition to $TiO_2$, the $ZrO_2$ semiconductor can also be used as an effective photocatalyst with a bandgap energy of 3.2–5.1 eV. $ZrO_2$ has high thermal stability, resistant to corrosion, non-toxic and eco-friendly [8-9]. But the recombination process decreases $ZrO_2$ photocatalytic efficiency. Efforts made to overcome this involves doping it with metal or coupling it with another semiconductor that has small $E_g$ so that it can prevent electron-hole recombination [10-11].

In this research, Cu-doped $ZrTiO_4$ material will be synthesized by sol-gel method. The advantages of this method are high purity of the products, low process temperature, the ability to control the resulted crystal phase, high resistance of the composites towards solvent as well as high thermal and mechanical stability [12-13]. Modification through sol-gel method has resulted in the formation of homogenous composites with smooth surface [14]. The parameters that would be investigated in this study were the Cu concentration and the calcination temperature.

## ■ EXPERIMENTAL SECTION

### Materials

Titanium(IV) isopropoxide (TTIP) (97%, Sigma-Aldrich) and zirconia powder ($ZrO_2$) (Jiaozuo Huasu) were used as precursors for synthesizing the photocatalyst material, copper(II) sulfate pentahydrate ($CuSO_4{\cdot}5H_2O$) (Merck), absolute ethanol (PA, Merck) and demineralized water (Jaya Sentosa) were used in sol-gel method.

### Instrumentation

X-ray powder diffraction (XRD) PANalytical X'Pert PRO MRD instrument with CuKα radiation was used to analyze the crystal structure. Fourier-Transform Infrared spectrophotometer (FT-IR) analysis was conducted using Thermo Nicolet iS10. Specular Reflectance UV-Vis spectrophotometer UV1700 Pharmaspec (SR-UV) was used to analyze the absorption of the materials. The morphology and the composition of elements in Cu-doped $ZrTiO_4$ were measured using Scanning Electron Microscope-Energy Dispersive X-Ray spectrometer (SEM-EDX) JSM-6510LA with an accelerating voltage of 2000 kV.

### Procedure

Synthesis of Cu-doped $ZrTiO_4$ through sol-gel method was done by adding 25 mL of absolute ethanol dropwise in 2.5 mL of TTIP and then stirred for 30 min. Next, $CuSO_4{\cdot}5H_2O$ salts (concentration of Cu dopant: 0, 1, 3, 5, 7, 9% (w/w)) and 1 g of $ZrO_2$ powder were dissolved together in 25 mL of demineralized water, then dropped slowly into the Ti precursor until the gel was formed [15]. It was then stirred again for 30 min. Afterward, the mixture was centrifuged for 1 h at 2000 rpm to separate the solid. The obtained solid was dried in the open air for 24 h and then heated at 80 °C for 24 h. Finally, the material was calcined at 500, 700 and 900 °C for 4 h. All materials were characterized by using XRD, FTIR, SRUV, and SEM-EDX.

## ■ RESULTS AND DISCUSSION

Fig. 1 shows the diffraction pattern of the Cu-doped $ZrTiO_4$ with various Cu concentrations after calcination at 500 °C. Characteristic peak of $TiO_2$ anatase (JCPDS: 01-084-1286) appeared at 25° ($d_{101}$) and 48° ($d_{200}$). On the other hand, $ZrO_2$ monoclinic (JCPDS: 01-088-2390) appeared in $ZrO_2$ reference at 28° ($d_{-111}$), 31° ($d_{111}$), 34° ($d_{002}$) and 51° ($d_{220}$). The anatase peak at 25° ($d_{101}$) showed a change in intensity along with Cu dopant concentration. The intensity of anatase decreased as copper concentration increased up to 5%, and became stagnant at above 5%. The copper dopant as impurity inhibits anatase transformation of $TiO_2$ from the amorphous sol-gel product.

Fig. 2 shows the diffraction pattern of 5% Cu-doped $ZrTiO_4$ calcined at various temperatures with the reference materials of $TiO_2$ and $ZrO_2$ after 500 °C calcination. The diffraction pattern of $TiO_2$ and $ZrO_2$ calcined at 500 °C indicates the presence of anatase and monoclinic phase. Cu-doped $ZrTiO_4$ after 900 °C calcination showed characteristic rutile pattern (JCPDS: 01-076-1938) at 27° ($d_{110}$), 36° ($d_{101}$), 41° ($d_{111}$) and 54° ($d_{211}$), while intensity of anatase pattern at 25° ($d_{101}$) and 48° ($d_{200}$) decreased. At 900 °C calcination, the Cu-doped $ZrTiO_4$ had an anatase peak intensity that decreased significantly in comparison at 700 °C; and the dominant

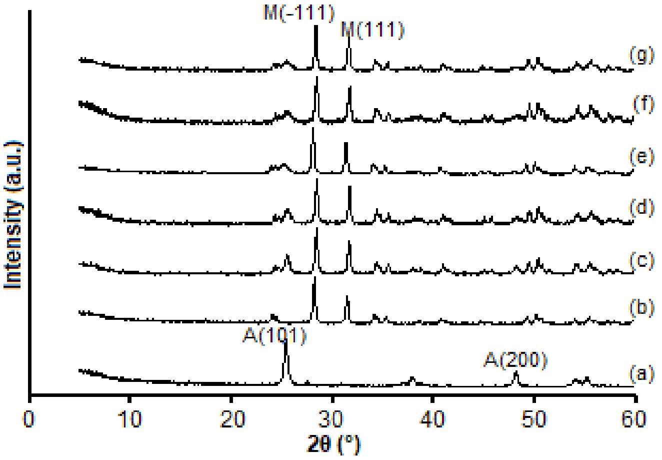

**Fig 1.** Diffraction pattern of (a) $TiO_2$, (b) $ZrO_2$, and Cu-doped $ZrTiO_4$ with (c) 1, (d) 3, (e) 5, (f) 7 and (g) 9% (w/w) of Cu concentration at 500 °C calcination

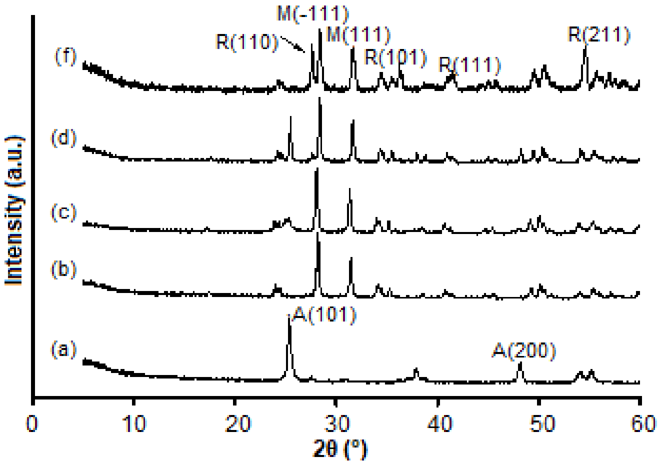

**Fig 2.** Diffraction pattern of (a) $TiO_2$ 500 °C, (b) $ZrO_2$ 500 °C and 5% Cu-doped $ZrTiO_4$ with (c) 500, (d) 700 and (e) 900 °C of calcination temperature

rutile phase at 900 °C. This proved that the existence of $ZrO_2$, which was dominant as supporting material, can inhibit anatase transformation to rutile [16].

Fig. 3 shows the FTIR spectra of materials with a various Cu dopant concentration in Cu-doped $ZrTiO_4$ along with $TiO_2$ and $ZrO_2$ as references. The characteristic peaks around 660 and 581 $cm^{-1}$ which are the vibrations of Zr–O and Ti–O bonds [17] tend to change as the $Cu^{2+}$ dopant concentration increased. This indicates that Cu metal was successfully doped on the photocatalyst surface.

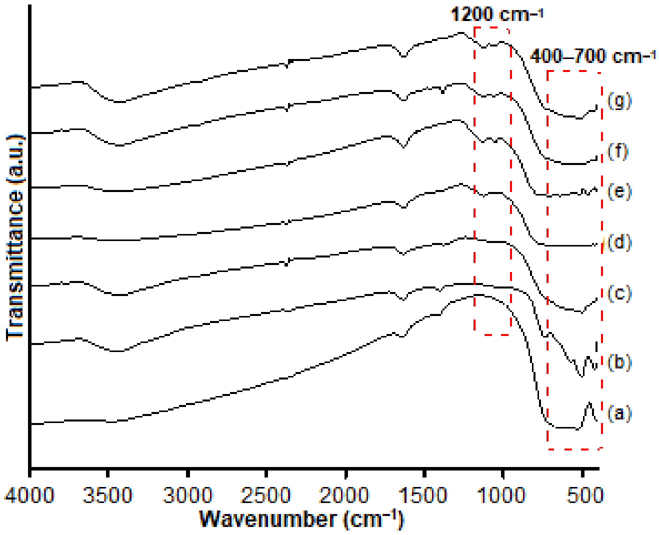

**Fig 3.** FTIR spectra of (a) $TiO_2$, (b) $ZrO_2$, and Cu-doped $ZrTiO_4$ with (c) 1, (d) 3, (e) 5, (f) 7 and (g) 9% (w/w) of Cu concentration at 500 °C calcination

Absorption at wavenumber 1635 and 3400 $cm^{-1}$ are the bending and stretching vibrations of $H_2O$ molecules. There is a vibrational bond that appeared around 1200 $cm^{-1}$ which shows the vibration of Cu–O–Zr via Ti–O–Zr bridge on the surface of $ZrO_2$. The peak intensity decreased from 3 to 5% Cu-doped $ZrTiO_4$. The peak intensity of Cu–O–Zr vibration increased as Cu concentration increased until 5% and stayed stagnant above 5%. It is believed that the excess Cu (above 5%) doped the $ZrTiO_4$ system at the interstitial position or possibly aggregating.

Fig. 4 shows the FTIR spectra of various calcination temperatures Cu-doped $ZrTiO_4$ together with $TiO_2$ and $ZrO_2$ as references. The peak showed the different intensity of Cu–O–Ti or Cu–O–Zr at the wavenumber of 400–700 and 1200 $cm^{-1}$ at different temperatures. The intensity decreased when the calcination temperature was 500 °C. The lowest intensity indicates that the material had been doped optimally. The characteristic peak of Ti–O–Ti bond changed at temperature 700 and 900 °C. This is caused by the transformation of anatase to rutile phase. The bond length between the anatase Ti–O phases is shorter than the rutile phase Ti–O, resulting in different vibrational energy.

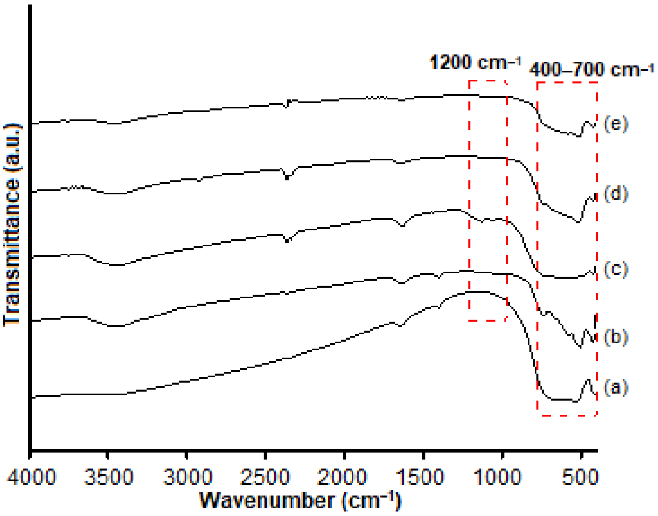

**Fig 4.** FTIR spectra of (a) $TiO_2$ 500 °C, (b) $ZrO_2$ 500 °C, and 5% Cu-doped $ZrTiO_4$ with (c) 500, (d) 700 and (e) 900 °C of calcination temperature

**Table 1.** Bandgap data of Cu-doped $ZrTiO_4$ with $ZrO_2$ and $TiO_2$

| Sample | $E_g$ (eV) |
|---|---|
| $ZrO_2$ 500 °C | 3.23 |
| $TiO_2$ 500 °C | 3.02 |
| Cu-$ZrTiO_4$ 1% 500 °C | 3.07 |
| Cu-$ZrTiO_4$ 3% 500 °C | 3.06 |
| Cu-$ZrTiO_4$ 5% 500 °C | 2.87 |
| Cu-$ZrTiO_4$ 5% 700 °C | 2.99 |
| Cu-$ZrTiO_4$ 5% 900 °C | 2.93 |
| Cu-$ZrTiO_4$ 7% 500 °C | 2.95 |
| Cu-$ZrTiO_4$ 9% 500 °C | 2.97 |

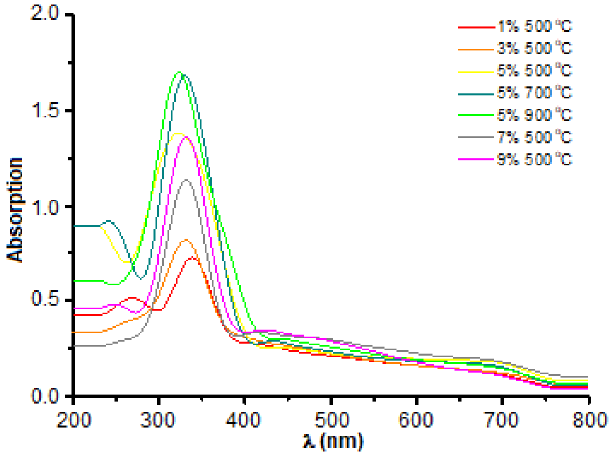

**Fig 5.** UV-Vis absorption spectra of various Cu-doped $ZrTiO_4$

Bandgap value of Cu-doped $ZrTiO_4$ with $ZrO_2$ and $TiO_2$ is shown in Table 1. Fig. 5 shows the absorption spectra of Cu-doped $ZrTiO_4$ together with the references. There is a shift in absorption from the wavelength of UV-light to the visible-light region. The $E_g$ value decreased as Cu concentration increased until the optimum condition of 5% with the lowest bandgap in which 2.87 eV. It is believed that the composite will have more responsivity towards solar irradiation. Higher the dopant concentration of Cu, greater the shift in absorption in comparison to the undoped $TiO_2$ and $ZrO_2$ [18]. While at Cu concentrations of 7 and 9%, the absorption returned to the lower wavelength. Thus the $E_g$ value increased because of the heterojunction effect. Higher calcination temperatures of 5% Cu increased the bandgap value due to sintering effect on the surface crystal of photocatalyst, so the dopant was not homogenously distributed and reduced the doping effect.

Fig. 6 presents SEM images and EDX spectra for 5% Cu-doped $ZrO_2$ and $ZrTiO_4$ at calcination temperature of 500 °C. The presence of Cu, Ti, Zr, and O are shown in Table 2. The mass percentage of Cu on $ZrTiO_4$ surface was higher than on $ZrO_2$ surface. The average particles diameter was around 2–5 µm. The Cu-doped $ZrTiO_4$ photocatalyst looked more homogenously distributed than Cu-doped $ZrO_2$.

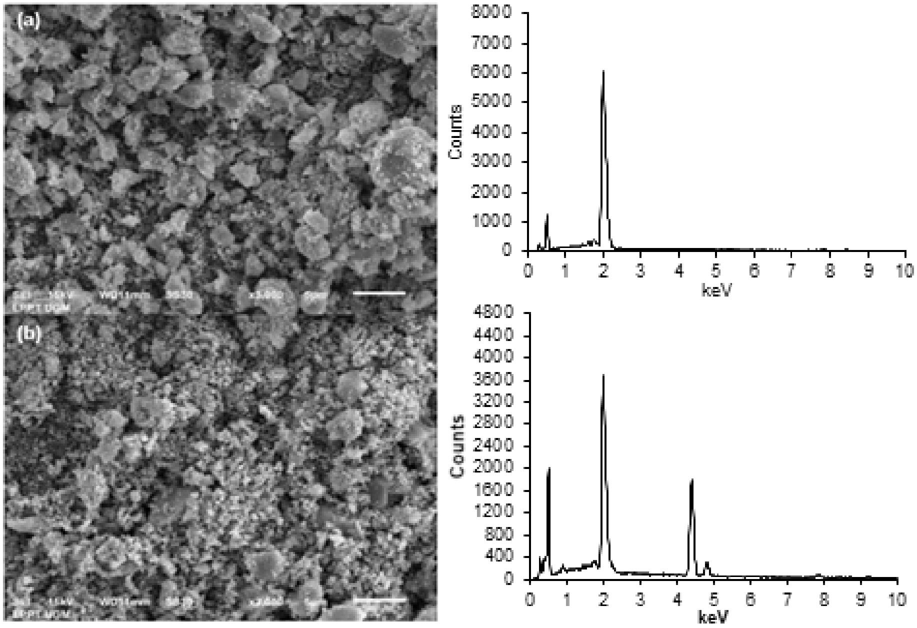

**Fig 6.** SEM images and EDX spectra of 5% Cu-doped (a) $ZrO_2$ and (b) $ZrTiO_4$ after calcination at 500 °C

**Table 2.** EDX analysis of 5% Cu-doped $ZrO_2$ and $ZrTiO_4$ after calcination at 500 °C

| Materials | % Mass | | | | |
|---|---|---|---|---|---|
| | Zr | O | Ti | Cu | Total |
| 5% Cu-doped $ZrO_2$ | 69.34 | 28.20 | - | 2.46 | 100 |
| 5% Cu-doped $ZrTiO_4$ | 35.22 | 38.44 | 23.02 | 3.31 | 100 |

## ■ CONCLUSION

Cu-doped $ZrTiO_4$ photocatalyst had been successfully synthesized by the sol-gel method. Cu metal dopants can affect the absorption shift of Cu-doped $ZrTiO_4$ to visible-light region if the added concentration does not exceed the optimum limit. The optimum concentration obtained at 5% of Cu concentration with $E_g$ value of 2.87 eV after calcination temperature of 500 °C with an absorption edge of 431.93 nm. Cu dopant inhibits the anatase formation at 500 °C calcination temperature. The presence of $ZrO_2$ can inhibit crystal transformation at high temperatures. The materials have better visible-light responsivity as a potential photocatalyst.

## ■ ACKNOWLEDGMENTS

We would like to express our gratitude for the financial support by DAMAS 2018 Grant (0244/J01.1.28/PL.06.02/2018) from the Faculty of Mathematics and Natural Sciences, Universitas Gadjah Mada, Indonesia.

## ■ REFERENCES

[1] Haider, A.J., Al-Anbari, R.H., Kadhim, G.R., and Salame, C.T., 2017, Exploring potential environmental applications of $TiO_2$ nanoparticles, *Energy Procedia*, 119, 332–345.

[2] Dunlop, P.S.M., Byrne, J.A., Manga, N., and Eggins, B.R., 2002, The photocatalytic removal of bacterial pollutants from drinking water, *J. Photochem. Photobiol., A*, 148 (1-3), 355–363.

[3] Qourzal, S., Assabbane, A., and Ait-Ichou, Y., 2004, Synthesis of $TiO_2$ via hydrolysis of titanium tetraisopropoxide and its photocatalytic activity on a suspended mixture with activated carbon in the degradation of 2-naphthol, *J. Photochem. Photobiol.*, 163 (3), 317–321.

[4] Yan, G., Zhang, M., Hou, J., and Yang, J., 2011, Photoelectrochemical and photocatalytic properties of N+S co-doped $TiO_2$ nanotube array films under visible light irradiation, *Mater. Chem. Phys.*, 129 (1-2), 553–557.

[5] Khairy, M., and Zakaria, W., 2014, Effect of metal-doping of $TiO_2$ nanoparticles on their photocatalytic activities toward removal of organic dyes, *Egypt. J. Pet.*, 23 (4), 419–426.

[6] Hu, Q., Huang, J., Li, G., Jiang, Y., Lan, H., Guo, W., and Cao, Y., 2016, Origin of the improved photocatalytic activity of Cu incorporated $TiO_2$ for hydrogen generation from water, *Appl. Surf. Sci.*, 382, 170–177.

[7] Luo, N., Jiang, Z., Shi, H., Cao, F., Xiao, T., and Edwards, P.P., 2009, Photo-catalytic conversion of oxygenated hydrocarbons to hydrogen over heteroatom-doped $TiO_2$ catalysts, *Int. J. Hydrogen Energy*, 34 (1), 125–129.

[8] Chang, S., and Doong, R., 2004, The effect of chemical states of dopants on the microstructures and band gaps of metal-doped $ZrO_2$ thin films at different temperatures, *J. Phys. Chem. B*, 108 (46), 18098–18103.

[9] Fathy, A., Elkady, O., and Abu-Oqail, A., 2017, Synthesis and characterization of Cu–$ZrO_2$ nanocomposite produced by thermochemical process, *J. Alloys Compd.*, 719, 411–419.

[10] Botta, S.G., Navio, J.A., Hidalgo, M., Restrepo, G.M., and Litter, M.I., 1999, Photocatalytic properties of $ZrO_2$ and Fe/$ZrO_2$ semiconductors prepared by a sol-gel technique, *J. Photochem. Photobiol., A*, 129 (1-2), 89–99.

[11] Pirzada, B.M., Mir, N.A., Qutub, N., Mehraj, O., Sabir, S., and Muneer, M., 2015, Synthesis, characterization and optimization of photocatalytic

activity of $TiO_2/ZrO_2$ nanocomposite heterostructures, *Mater. Sci. Eng., B,* 193, 137–145.

[12] Esposito, S., Turco, M., Bagnasco, G., Cammarano, C., Pernice, P., and Aronne, A., 2010, Highly dispersed sol-gel synthesized Cu-$ZrO_2$ materials as catalysts for oxidative steam reforming of methanol, *Appl. Catal., A*, 372 (1), 48–57.

[13] Chen, Q., Chang, Y., Shao, C., Zhang, J., Wang, J.M., and Long, Y., 2014, Effect of grain size on phase transformation and photoluminescence property of the nanocrystalline $ZrO_2$ powders prepared by sol-gel method, *J. Mater. Sci. Technol.*, 30 (11), 1103–1107.

[14] Syoufian, A., Manako, Y., and Nakashima, K., 2015, Sol-gel preparation of photoactive srilankite-type zirconium titanate hollow spheres by templating sulfonated polystyrene latex particles, *Powder Technol.*, 280, 207–210.

[15] Andita, K.R., 2018, Synthesis of Cu-Doped $ZrTiO_4$ with Various Percentage of Cu and Calcination Temperatures as a Model of Visible-Light Responsive Photocatalyst, *Undergraduate Thesis*, Department of Chemistry, Universitas Gadjah Mada, Yogyakarta.

[16] Nankya, R., and Kim, K.N., 2016, Sol-gel synthesis and characterization of Cu–$TiO_2$ nanoparticles with enhanced optical and photocatalytic properties, *J. Nanosci. Nanotechnol.*, 16 (1), 11631–11634.

[17] Agorku, E.S., Kuvarega, A.T., Mamba, B.B., Pandey, A.C., and Mishra, A.K., 2015, Enhanced visible-light photocatalytic activity of multi-elements-doped $ZrO_2$ for degradation of indigo carmine, *J. Rare Earths*, 33 (5), 498–506.

[18] Choi, J., Park, H., and Hoffmann, M.R., 2010, Effects of single metal-ion doping on the visible-light photoreactivity of $TiO_2$, *J. Phys. Chem. C*, 114 (2), 783–792.